Muonic x rays in lead isotopes*

D. Kessler, H. Mes,† and A. C. Thompson‡
Carleton University, Ottawa, Canada K1S 5B6

H. L. Anderson and M. S. Dixit§
Enrico Fermi Institute, University of Chicago, Chicago, Illinois 60637

C. K. Hargrove and R. J. McKee
National Research Council of Canada, Ottawa, Canada K1A OR6

(Received 30 September 1974)

Results of an experiment to measure muonic transition energies in separated lead isotopes are presented. The main results are as follows: 1. Muonic spectra of the four lead isotopes ^{204}Pb, ^{206}Pb, ^{207}Pb, and ^{208}Pb were studied with high resolution. No anomalous splitting or broadening of the lines was detected. The effect of the natural linewidth could, however, be observed. 2. An anomaly was found in the $3d$ fine structure splitting whose measured value turned out to be larger than the calculated value by nearly 300 eV (or 10 standard deviations) in all four isotopes. 3. Except for this anomaly, the lower levels of muonic lead can be described adequately with the help of a two-parameter Fermi distribution of the nuclear charge. There is no evidence in the x-ray data for a central depression in the nuclear density. 4. We determine the nuclear polarization in the ground state of all four isotopes of lead and find values ranging from -7.3 ± 2.2 to -10.1 ± 1.1 keV, which are somewhat higher than, but not inconsistent with, the best theoretical predictions of -6.8 ± 2.0 keV. This analysis is made possible by our ability to measure the weak transitions involving the $2s$ level. 5. We find a slight and regular increase in nuclear density, going from ^{204}Pb to ^{208}Pb. The skin-thickness parameter t appears, however, to be practically the same in all four isotopes measured.

[RADIOACTIVITY ^{204}Pb, ^{206}Pb, ^{207}Pb, ^{208}Pb; muonic atoms, measured transition energies, levels up to $6f$; observed natural linewidth of L lines; observed anomalous fs splitting of $3d$; deduced Fermi parameters; deduced nuclear polarization of ground state.]

I. INTRODUCTION

In this paper, we present the results of a high precision experiment designed to study the muonic x rays from separated lead isotopes ^{204}Pb, ^{206}Pb, ^{207}Pb, and ^{208}Pb. This new experiment is a continuation of a previous experiment[1] in which only the latter three isotopes were studied, with particular emphasis on ^{206}Pb. The present experiment was intended to provide answers to specific questions which arose from this work. A substantial improvement over previous work was made possible by the availability of relatively large amounts of separated lead isotopes[2] and the achievement of higher resolution and precision than was possible before, using techniques which will be described in Sec. II. The experiment was performed using the muon beam of the University of Chicago synchrocyclotron a short time before it was dismantled.

The results of the experiment were presented in preliminary form before.[3] Since that time it was discovered,[4,5] however, that one of the corrections to the muonic energy levels, namely the higher order vacuum polarization, was not given correctly in the literature. Only recently did the correct values for these corrections become available,[6] so that our data could be reanalyzed. The results will be described in this paper.

We will now describe in more detail the main problems which motivated this investigation:

1. *Search for a possible structure of the x-ray lines due to nuclear effects.* This possibility arises from the strong coupling between the muon and the nucleus, especially in heavy elements. As an example of such an effect, we may mention the so-called *prompt* γ rays which we discovered in the lead spectra several years ago.[7] These γ rays, as their name implies, differ from the common capture γ rays in that they appear only in the prompt spectrum, and not in the delayed one. In addition, whereas the capture γ rays always belong to isotopes of the element with atomic number $Z-1$, the prompt γ rays belong to isotopes of the target element Z. For instance, in the prompt spectrum of ^{207}Pb, we identified characteristic lines of excited ^{207}Pb and ^{206}Pb. We interpret the process responsible for these *prompt* γ rays as "inverse internal conversion," whereby the nucleus is being excited by a radiationless transi-

tion of the orbital muon from a higher excited state to the 1*s* state. The nucleus then decays to the ground state with or without neutron emission. In a subsequent experiment we were able to detect such neutrons emitted during deexcitation of the muonic atom.[8] Processes of this type are relatively frequent, they occur in about 5–10% of all muon stops in the target and imply a rather tight coupling between the orbital muon and the nucleus. We therefore planned to look at the lines, especially the *K* lines, with the best possible resolution in order to detect any possible structure due to this kind of interaction.

2. *Investigation of the isotope shifts in* $^{204,206,207,208}Pb$. In I, only the isotopes 206, 207, and 208 were investigated. The main result was the observation that, in going from the lighter to the heavier isotopes, the isotope shifts are only about half as large as one would predict from an assumed $A^{1/3}$ variation of the nuclear radius. In other words, adding one or two neutrons to ^{206}Pb produces an increase in the nuclear radius, but not as much as one would expect if the density remained the same. In fact, our measurements show that the density increases slightly as one approaches the double magic nucleus ^{208}Pb, in agreement with optical[9] and electronic x-ray results.[10,11] In the present experiment we set out to repeat these measurements with higher precision and, moreover, to extend them to the isotope ^{204}Pb which has never been measured before. We were fortunate to obtain comparatively large quantities of separated isotopes on loan[2] and the measurements for all four lead isotopes were performed concurrently.

The study of isotope shifts is not the only reason for using separated isotopes. As will be shown, there are problems of interpretation due to inadequacies of the model used to describe the data. The amount of information available from one isotope is usually insufficient by itself to discriminate between different models, but a comparison of different isotopes can often provide a clue to the correct interpretation.

3. *Precise measurement of the 2s levels in all four isotopes.* As is well known, the lines which appear strongly in the muonic x-ray spectrum are the $K\alpha$, $L\alpha$, etc., lines. These lines are strong due to peculiarities in the cascade process which preferentially populates the circular orbits. They are shifted from their point-nucleus energies due to finite-size effects and have been used, therefore, to study nuclear sizes and shapes ever since Fitch and Rainwater performed their pioneer experiment.[12] The information provided by these lines is sufficient to determine one nuclear parameter (namely, the rms radius) in light nuclei and an additional parameter (the skin thickness) in medium and heavy nuclei. Seven years ago, we observed for the first time transitions involving the 2*s* state.[13] Since that time we have tried on every occasion to observe these transitions and to make use of the additional information they provide. The problem here is that these lines are very weak, since the population of the 2*s* state is only of the order of a few percent in light elements and goes down to about 1% in lead. The observation of transitions to and from the 2*s* level, therefore, requires both high statistics and good resolution.

The importance of the 2*s* level is illustrated in Fig. 1.[14] This figure shows how the muon in its various orbits penetrates the nucleus. The dashed line is the charge distribution in lead and one notices how the 1*s* wave penetrates the nucleus, while the 2*p* waves penetrate much less and 3*d* hardly at all. The 2*s* wave, on the other hand, has the largest overlap with the nucleus, next to the ground state. (Note that 2*s* is drawn to the same scale as 1*s*, whereas the 2*p* curves are scaled up by a factor 10.) It should be pointed out, nevertheless, that the sensitivity of muonic atom measurements to nuclear size effects is determined by the overlap integrand $(f^2+g^2)\rho(r)r^2$, where f and g are the two components of the radial solutions to the Dirac equation. In lead this integrand rises from zero at the center of the nucleus to a maximum which is at about 4.2 fm for 2*s*, 5.3 fm for 1*s*, and 5.8 fm for the 2*p* waves.

An interesting property of 2*s* is that it happens to have a zero at the fringe of the lead nucleus so that, discounting the remote possibility of a nuclear halo reaching out to twice the rms radius, one sees that 2*s* is sensitive exclusively to the

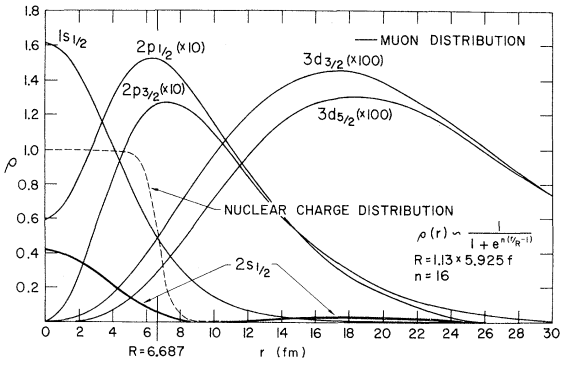

FIG. 1. Muon and nuclear charge distributions in lead ($Z=82$). The muon is represented by the square of the wave function $|\psi|^2$, where $\int|\psi|^2r^2dr=1$. The nuclear charge distribution is of the Fermi type, calculated using the parameters shown in the figure.

interior of the charge distribution. This is further illustrated on a so-called c-t plot, Fig. 2. The lines are isoenergetic lines drawn for the actually observed muonic energy levels in lead. Each line connects those values of the nuclear parameters c and t which lead to the observed energy of a particular level. [For a definition of c and t see Eqs. (2) and (4).] The lines corresponding to various states all intersect in one point whose coordinates are the actual values of c and t. It is immediately apparent from the figure that the isoenergetic line for the $2s$ level is flatter than all the others, that is, less dependent on the skin-thickness parameter t. The ground state comes next, and higher angular momentum states show a gradually increasing dependence on t, in accord with the fact that their overlap with the nucleus peaks further and further out in the nuclear fringe.

We previously used the additional information supplied by the measurement of the $2s$ level in ^{206}Pb to provide, for the first time, evidence for the existence of nuclear polarization by the muon.[1,15] The argument ran as follows: Whereas it is possible to fit the K and L lines and their fine-structure splitting with a two-parameter Fermi shape, one does no longer obtain a good fit if one uses in addition the $3p$-$2s$ and $2s$-$2p$ energies. However, one has now sufficient information to determine the nuclear parameters *without* making use of the $K\alpha$ line. If one then uses these parameters to calculate the $K\alpha$ energy, one finds a difference between the calculated and experimental $2p$-$1s$ energies. This difference amounted to 6.8 ± 2.3 keV in our previous work,[15] in good agreement with the most up-to-date theoretical calculations[16,17] then available, which gave a nuclear polarization correction to the $1s$-binding energy of 6 keV ($\pm 50\%$).

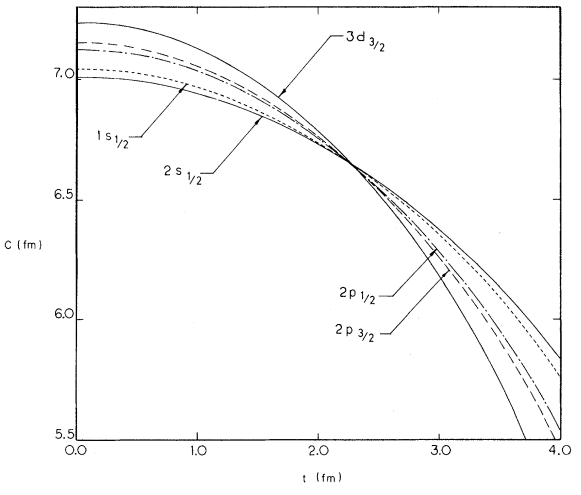

FIG. 2. c-t plot for the lower energy levels in lead.

The lack of a consistent set of theoretical nuclear polarization corrections prevented us at the time from applying these corrections to the higher levels. Our result, therefore, could not be considered as a measurement of nuclear polarization, but only as a demonstration that a discrepancy suggestive of nuclear polarization is present. It was one of the objectives of the present experiment to pursue this problem further by analyzing all four lead isotopes simultaneously. The results, already reported in preliminary form,[3] show that nuclear polarization is present in all four isotopes in roughly the amount predicted by theory. Jenkins *et al.*[18] using both $2s$ lines reported a similar agreement in ^{208}Pb, following essentially the same method, but with inclusion of the nuclear polarization corrections in the higher levels.

Section II describes the experimental techniques. Section III deals with line shapes. The lower energy levels of the four lead isotopes are determined in Sec. IV. This section also contains a discussion of the isotope shifts. In Sec. V we discuss the nuclear charge parameters in the lead isotopes and the related problem of nuclear polarization. Section VI summarizes the conclusions.

II. EXPERIMENTAL TECHNIQUES

A. Muon telescope

The forward muon beam of momentum 150 MeV/c from the muon channel of the University of Chicago synchrocyclotron was used a short time before the latter was dismantled. The muon telescope was of a conventional type, similar to that used in I, and is shown in Fig. 3. The muon beam was defined by three counters in front of the target. An anticoincidence counter behind the target vetoed particles passing through. Electrons present in the beam were vetoed using a Cerenkov counter. A polyethylene moderator was used to remove the pions and its thickness was adjusted so as to maximize the number of muons stopping in the target.

Up to four different targets could be measured simultaneously by subdividing the target area into four parts. Each individual target was about 10×10 cm^2, 4 g/cm^2 thick, and separated from its neighbors by ledges of the veto counter to avoid cross talk. Scintillation counters placed flat in front of each target were used to label muons stopping in any one of the four targets.

B. Spectrometer

The spectrometer consisted of a Ge(Li) detector, preamplifier, amplifier, and a 13-bit analog-to-digital converter (ADC) with digital stabilization. In addition, a mercury relay pulse generator

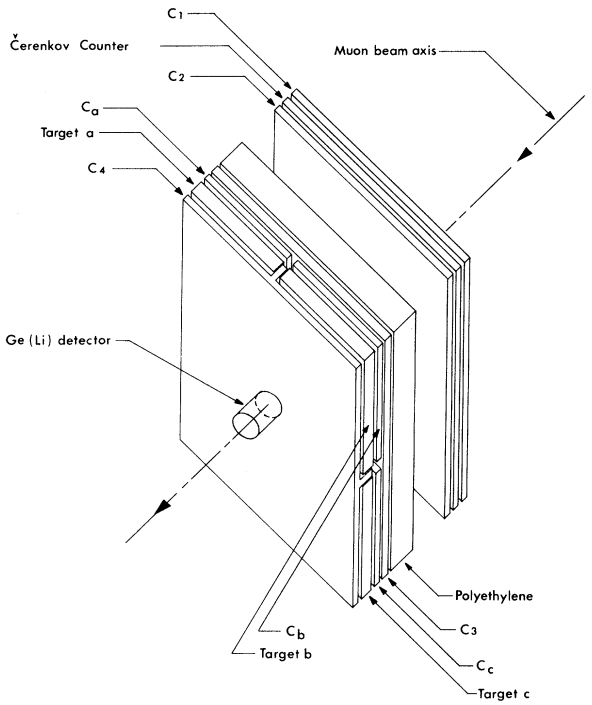

FIG. 3. Schematic view of the muon telescope and detector.

whose amplitude was distributed over the spectrum by a computer-controlled 15-bit digital-to-analog converter (DAC pulser) was used to measure the linearity of the system concurrently with the data.

The measurements were carried out using an Ortec 25 cm^3 coaxial lithium drifted germanium detector. The measured system resolution with the beam on was 3.0 keV for the 1.33 MeV ^{60}Co line and 7.2 keV for the 6.13 MeV $^{16}O^*$ line.

The linear signal from the amplifier was gated into the ADC when the appropriate logic conditions for an x ray, delayed γ ray, source, pulser, or DAC event were satisfied. The ADC sent an interrupt to the computer after it had finished digitizing. The computer disabled further interrupts, then read and reset the 13-bit ADC, as well as the tag register (which identified the origin of the pulse) and the 8-bit ADC which was used to measure the time of arrival of the γ-ray pulse with respect to the muon stop in the target. This information was put into a temporary buffer after which the interrupt facility was again enabled. The time interval between interrupts was used to histogram the data into spectra of target events, source events and DAC events, using the information from the tag register.

The classification of a pulse as a prompt x ray or a delayed γ ray was based on timing. Since the Ge(Li) detector timing was dependent on the pulse amplitude, the computer made use of a resident look-up table which correlated the timing information with the pulse amplitude to classify the event as a prompt x ray or a delayed γ ray.

In order to achieve the highest possible resolution, it is necessary to match the high intrinsic resolution of the detector with high stability and precise calibration of the electronic system.

Stability was achieved by the standard method of digitally stabilizing the zero level and the gain of the ADC. The stabilizers were operated on two pulser peaks. One was set low to stabilize the zero level, the other was set high to stabilize the gain. These two fixed pulsers were powered by a highly stable power supply and they were driven at 50 cps under computer control.

The problem of calibration, on the other hand, was solved using a novel method, which has already been described elsewhere in great detail.[19] The conventional method of calibrating a spectrometer system consists of using a precision pulse generator and digital voltmeter along with a set of standard γ-ray sources. This method provides a certain number of precisely calibrated points to which one fits a gain correction curve. This curve serves to correct the data for nonlinearities in the system. The disadvantage of this approach is that it requires interpolation between the calibration points, so that the precision one can achieve varies along the spectrum, being higher close to the calibration points and much lower midway inbetween. In order to overcome this difficulty, we used in this experiment an improved version of a sliding pulser system developed by Strauss, Lenkszus, and Eicholz.[20] In our system, the sliding pulser was replaced with a mercury relay pulse generator whose amplitude was controlled by a 15-bit DAC under computer control. This DAC, manufactured by Analog Devices, has a linearity rated at $\pm\frac{1}{2}$ of the least significant bit, or 15 ppm. Checking the linearity of the DAC against a six-digit DVM, we found a rms deviation of less than 7 ppm.

The DAC was stepped throughout the range of the spectrum keeping the number of counts at each setting constant. The DAC pulses were fed through the same chain of preamplifier, amplifier, and ADC as the Ge(Li) detector pulses and provided therefore a differential response curve for the whole system. This method has the advantage of linearizing the electronics in a model-independent way and, since it can be shown[19] that under ideal conditions the integral of the DAC spectrum is linear with the DAC setting and therefore linear with energy, the data are automatically calibrated.

A small deviation from linearity can occur due

to electronic noise. This effect has been analyzed in detail by McKee *et al.*[19] who have shown that the deviation from linearity is negligible if the noise is kept reasonably small. It was shown, however, that the presence of background may produce some distortions if no precautions are taken. Here the background is produced by accidental coincidences between pulser events and detector events, since the data and DAC spectrum are collected simultaneously. This effect was reduced to a large extent by introducing a DAC window, which is a requirement that the pulser count fall in a channel range centered at the channel corresponding to the DAC setting. It was also shown that the error introduced by the window is negligible unless the background is very large or the window width is excessive. More important than these systematic errors are statistical errors which arise from the fact that the pulser peak distribution has a finite width. These effects were also analyzed in detail by McKee *et al.*[19] As usual, the effect of these errors can be made small by increasing the statistics. An expression is given in the paper quoted for the number of DAC cycles necessary to achieve a given precision. In our experiment the number of DAC cycles in each run, typically a few hundred, was kept well above the calculated limit.

The source lines which were used for energy calibration are listed in Table I.

III. LINE SHAPES

In Sec. I, we gave some reasons for examining the x-ray lines for a possible structure or anomaly. Some examples of the spectra observed will be shown in the following figures. Figure 4 shows the single escape (SE) and double escape (DE) K lines. Figure 5 shows two of the L lines in double escape. In the same figure, we see a triplet of $5f$-$3d$ lines

TABLE I. Source energies.

γ-ray source	Adopted energy (keV)	γ-ray source	Adopted energy (keV)
^{88}Y (DE)	814.12 ± 0.04 [a]	^{56}Co	1771.48 ± 0.06 [b]
^{56}Co	846.75 ± 0.04 [b]	^{88}Y	1836.13 ± 0.04 [a]
^{88}Y	898.04 ± 0.04 [a]	^{56}Co	2598.55 ± 0.04 [b]
^{56}Co	1037.90 ± 0.05 [b]	^{228}Th	2614.49 ± 0.09 [g]
^{56}Co, ^{60}Co	1173.26 ± 0.03 [b-d]	^{56}Co (SE)	2742.62 ± 0.05 [b]
^{56}Co	1238.31 ± 0.03 [b]	^{24}Na	2754.10 ± 0.09 [e,f]
^{60}Co	1332.51 ± 0.03 [c]	^{16}O (DE)	5107.3 ± 0.4 [a]
^{56}Co	1360.27 ± 0.04 [b]	^{16}O (SE)	5618.3 ± 0.4 [a]
^{24}Na	1368.53 ± 0.04 [e]	^{16}O	6129.3 ± 0.4 [a]
^{56}Co (DE)	1576.54 ± 0.04 [b]	^{16}O (DE)	6093.4 ± 0.4 [h]
^{228}Th (DE)	1592.48 ± 0.09 [g]	^{16}O (SE)	6604.4 ± 0.4 [h]
^{24}Na (DE)	1732.09 ± 0.09 [e,f]	^{16}O	7115.4 ± 0.4 [h]

[a] J. B. Marion, Nucl. Data A4, 301 (1968).

[b] M. N. Rao, Nucl. Data B3, 43 (1970). The adopted energies found in this reference were adjusted slightly by fitting the 23 transition energies to the 12 energy levels involved in the transitions, taking the recoil of the ^{56}Co nucleus into account.

[c] Weighted average from the following references: G. Murray, R. L. Graham, and J. S. Geiger, Nucl. Phys. 63, 353 (1965); R. K. Smither and A. I. Namenson, quoted in J. B. Marion, University of Maryland, Department of Physics and Astronomy Technical Report No. 653, 1967 (unpublished); J. J. Reidy and M. L. Wiedenbeck, Bull. Am. Phys. Soc. 10, 1131 (1965); D. H. White and D. J. Grover, Nucl. Phys. A91, 453 (1967); J. J. Reidy, unpublished.

[d] This is a composite of the 1173.227 ± 0.030 keV line of ^{60}Co and the 1175.16 ± 0.05 keV line of ^{56}Co (see references c and b, respectively). The fraction contributed by ^{56}Co was taken to be $w = 0.016 \pm 0.003$, obtained by using three nearby ^{56}Co lines. The relative intensities of the ^{56}Co lines are given in Ref. b. The counter efficiency at the composite peak was found by quadratic interpolation using the three nearby ^{56}Co lines. A 20% uncertainty on w was assumed. The energy of the composite line was calculated from $E = (1-w)E(^{60}\text{Co}) + wE(^{56}\text{Co})$.

[e] G. Murray, R. L. Graham, and J. S. Geiger, Nucl. Phys. 63, 353 (1965).

[f] R. Gunnick, R. A. Meyer, J. B. Niday, and R. P. Anderson, Nucl. Instrum. Methods 65, 26 (1968).

[g] Weighted average between Ref. e and *Nuclear Data Tables*.

[h] Obtained using Ref. a and the splitting 6129(FE)-7115(DE) = 35.90 ± 0.15 keV of D. E. Allburger, private communication.

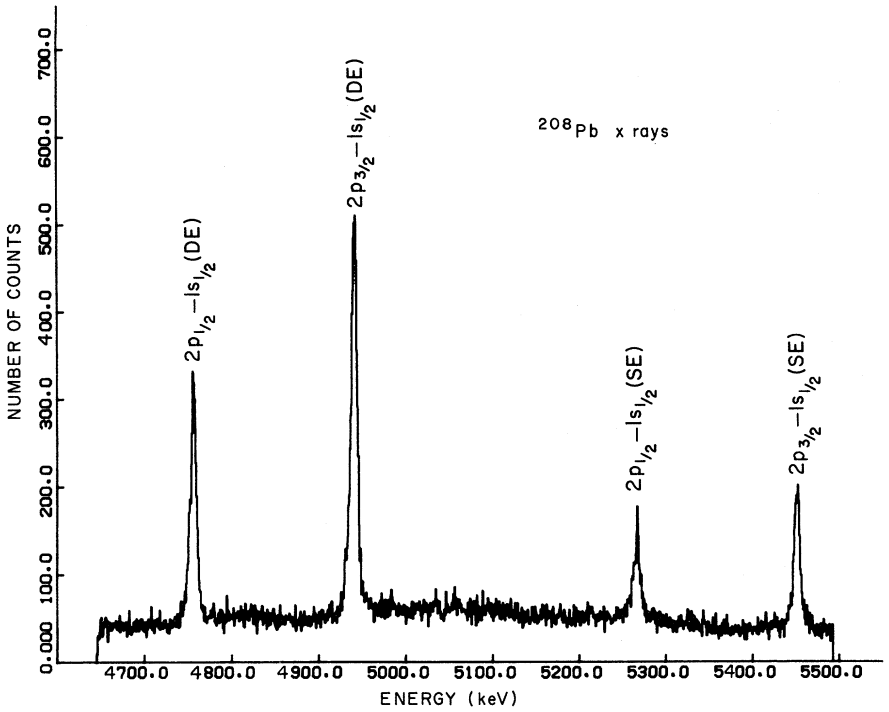

FIG. 4. ^{208}Pb K lines in single and double escape.

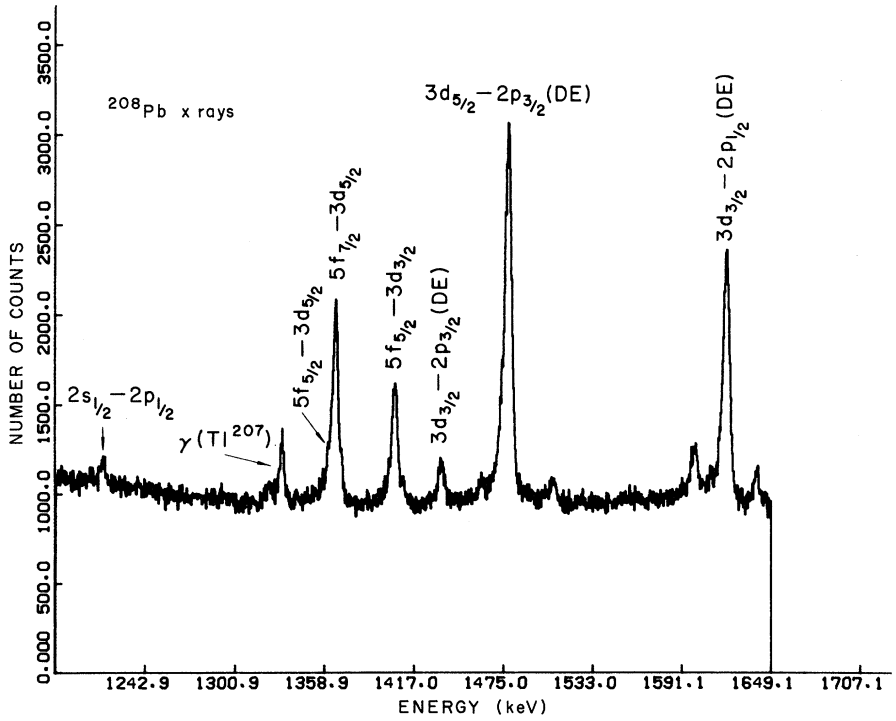

FIG. 5. ^{208}Pb double escape L lines. Also shown is the $5f$-$3d$ triplet, a capture γ ray, and a $2s$-$2p$ line.

as well as a capture γ ray, identified as belonging to ^{207}Tl. The small peak on the left belongs to the transition $2s_{1/2}$-$2p_{1/2}$. This is one of those weak transitions involving the $2s$ state which we set out to observe and which will be discussed in Sec. V. Another such transition, the $2s_{1/2}$-$2p_{3/2}$ transition, is shown in Fig. 6, along with a triplet of M lines.

A close examination of the line shapes reveals no structure nor anomaly. This is all the more remarkable since our resolution is good enough to detect the *natural width* of these lines. Measurements of the natural line width in muonic x rays were first performed by our group in a related experiment[21,22] on higher transitions, such as $5g$-$4f$, in lead and lighter elements. We observe, indeed, that most x ray lines in lead are consistently wider than source peaks of comparable energy.

The full width at half-maximum (FWHM) of the measured x-ray peak Γ_m is related to the natural (Lorentzian) width Γ_n and the instrumental resolution Γ_i, assumed to be Gaussian, by the following relation[23]

$$\Gamma_n = \Gamma_m - \Gamma_i^2/\Gamma_m \,. \tag{1}$$

The FWHM of the L lines, for instance, turns out to be 5.0 keV, whereas our resolution in the same energy region, as derived from the width of the source peaks, is about $\Gamma_i = 3.9$ keV.

The natural width Γ_n of the L lines can be calculated. It is given by the sum of the Γ's of the $3d$ and $2p$ levels, which in turn are related to the transition rates. Care must be taken in calculating these transition rates, since the usual approximation which consists in using point-nucleus wave functions for the dipole matrix element, while taking the exact transition energy into account in the E^3 factor is inadequate here. As pointed out to us by Sundaresan[24] the dipole matrix element in lead is increased by more than a factor of 2 over the point-nucleus value. The calculated transition rates for the $3d$-$2p$ and $2p$-$1s$ transitions in lead are, respectively, of the order of 0.6×10^{18} and 2.0×10^{18} sec^{-1}. The corresponding widths of the $3d$ and $2p$ levels are 0.4 and 1.4 keV, respectively, so that the natural width of the $3d$-$2p$ lines is expected to be about $\Gamma_n = 1.8$ keV. Solving Eqs. (1) for the predicted experimental line width, one obtains $\Gamma_m = 4.9$ keV, in good agreement with the observed value of 5.0 keV.

Our work on the $5g$-$4f$ transitions in lead, as well as higher transitions in some lighter elements, will be described in a separate paper.[25]

IV. MEASURED ENERGIES AND ISOTOPE SHIFTS

The isotopic composition of the four lead targets is listed in Table II. Target II was made up of

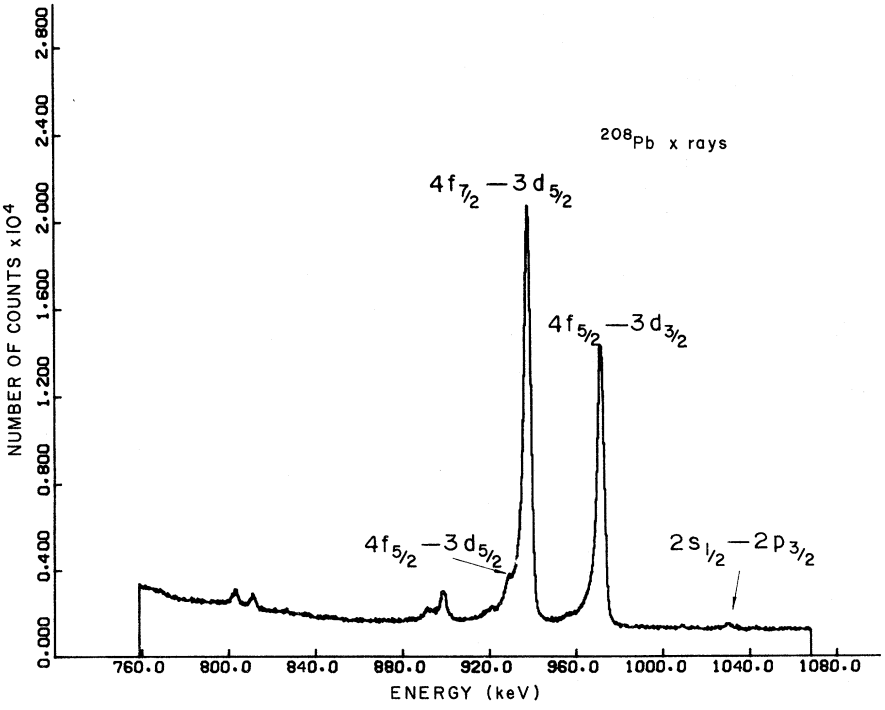

FIG. 6. ^{208}Pb full energy M lines and the $2s_{1/2}$-$2p_{3/2}$ line.

TABLE II. Composition of targets.

Target	Isotopic composition (%) 208	207	206	204	Weight (g)
I "Pb-208"	98.7	1.0	0.3	0.0	498.0
II "Pb-207"	9.9	87.5	2.6	0.0	477.1
III "Pb-206"	2.7	8.5	88.7	0.1	1453.0
IV "Pb-204"	10.0	6.4	12.7	70.9	99.5

two slabs of somewhat different isotopic composition placed side by side. The composition quoted in the table is a weighted average of the two compositions, taking into account the distribution of muon stops.

The measured values of the $K\alpha$ lines of the four lead isotopes are shown in Table III. The fine-structure splitting is listed separately, since it can be measured much more accurately than the absolute value of the energy of each component of the doublet. Also listed are two weak $K\beta$ transitions, namely, $3p$-$1s$ and $3d$-$1s$. The latter transition is an $E2$ transition.

Table IV shows the L lines and their fine-structure splitting. The difference between the $2p$ and $3d$ splittings can be determined with high precision directly from the energy difference of the two strong components of the triplet. The individual splittings, however, require all three energies and cannot be determined with the same degree of accuracy. It should be pointed out that in this table, as well as in Table V, errors of less than 60 eV were arbitrarily increased to 60 eV to account for the possibility of systematic errors.

Table V lists the measured energies of the M lines. Only the two strong lines of each triplet are shown in the table, because the weak third line was barely resolved and could therefore not be measured independently. In the line fitting procedure its distance to the nearest line was constrained to its theoretical value.

Since we measure three triplets, namely, $M\beta$ and $M\gamma$ as well as $M\alpha$, we can determine the $3d$ splitting in three ways. To do this, one uses the two strong and well separated lines which yield the difference $\Delta(3d) - \Delta(nf)$ between the fine-structure splitting of the $3d$ levels and that of the upper nf levels ($n = 4$, 5, and 6). The $3d$ splitting is derived from this quantity by assuming the calculated value for $\Delta(nf)$. This is permissible, since the $4f$ and higher splittings are small and can be calculated accurately in a model-independent way. The results are shown in Table V along with the values of the $3d$ splittings obtained directly from the triplet of $L\alpha$ lines, as listed in Table IV. The four values for each isotope agree reasonably well, as do the mean values for the four isotopes. The over-all average for the $3d$ splitting is 43.12 ± 0.02 keV with a $\chi^2/N = 2.2$. This high value of χ^2 may indicate that some of the errors, in particular the small errors on the $3d$ splitting deduced from the $4f$-$3d$ lines, are underestimated. On the other hand, one cannot rule out the possibility that there are small but significant differences between the $3d$ splittings of the four isotopes, although the absence of a systematic trend does not make it appear very likely. In spite of this small inconsistency, it is clear, however, that the experimental values of the $3d$ splitting are significantly higher than the calculated value of 42.82 keV.

It should be noted that $5f$-$3d$ and $6f$-$3d$ could be contaminated by $E2$ transitions, such as $5g$-$3d$. This kind of contamination would, however, not affect the L lines, nor the $4f$-$3d$ lines. As can be seen from Table V, the latter provide by far the best determination of the $3d$ splitting.

One may wonder whether the discrepancy between the calculated and measured values of the $3d$ splitting $\Delta(3d)$ is a result of the way it has been determined using the M lines and constraining $\Delta(nf)$ to its calculated value. We have therefore attempted to fit the three $4f$-$3d$ energies for both $\Delta(3d)$ and $\Delta(4f)$. As shown at the bottom of Table V, the $3d$ splitting now tends to agree with the theoretical value within the rather large error of the fit. The $4f$ splitting, however, then disagrees substantially with its calculated value and furthermore, the $3d$ splitting determined directly from

TABLE III. K lines. Transition energies in keV.

	^{208}Pb	^{207}Pb	^{206}Pb	^{204}Pb
$2p_{1/2}$-$1s_{1/2}$	5777.91 ± 0.40	5783.79 ± 0.44	5787.00 ± 0.41	5796.06 ± 0.41
$2p_{3/2}$-$1s_{1/2}$	5962.77 ± 0.42	5968.89 ± 0.44	5972.80 ± 0.41	5982.12 ± 0.41
$2pfs$ splitt.	184.83 ± 0.10	185.09 ± 0.14	185.75 ± 0.06	186.04 ± 0.11
$3d_{3/2}$-$1s_{1/2}$	8419.51 ± 0.75	8426.42 ± 0.78	8430.85 ± 0.79	8442.11 ± 0.91
$3p_{3/2}$-$1s_{1/2}$	8501.53 ± 0.97	8507.52 ± 0.82	8512.15 ± 0.72	8523.30 ± 0.78

TABLE IV. L lines. Transition energies in keV.

	^{208}Pb	^{207}Pb	^{206}Pb	^{204}Pb
$3d_{3/2}$-$2p_{3/2}$	2457.20± 0.20	2457.86± 0.15	2458.33± 0.36	2459.70± 0.21
$3d_{5/2}$-$2p_{3/2}$	2500.33± 0.06	2501.10± 0.06	2501.60± 0.06	2502.83± 0.06
$3d_{3/2}$-$2p_{1/2}$	2642.11± 0.06	2642.93± 0.06	2644.14± 0.06	2645.52± 0.07
$2p$-$3d$ splitt.	141.77± 0.06	141.82± 0.08	142.53± 0.05	142.68± 0.08
$2p$ splitt.	184.89± 0.25	185.05± 0.17	185.76± 0.40	185.82± 0.22
$3d$ splitt.	43.13± 0.18	43.25± 0.13	43.24± 0.36	43.13± 0.21

the $L\alpha$ lines still disagrees both with the calculated value and with the fitted value deduced from the M lines. We therefore believe that the discrepancy in the $3d$ splittings is genuine, especially as it shows up consistently in all four isotopes.

There does not seem to be a ready explanation for the anomaly in the $3d$ splitting since it is insensitive to nuclear effects, such as size and shape parameters or nuclear polarization. It is possible that the discrepancy is related to the discrepancy observed in the higher transitions, which is discussed in separate papers,[21,22,25] but what causes these discrepancies is still an open question.

It is interesting to note that there was already some indication of the anomalous $3d$ splitting in older data, although with the errors quoted it was barely significant and was not at the time recognized as an anomaly. In particular, in I the $3d$ splitting of ^{208}Pb was found to be larger by 0.39 keV than the calculated value, while the error on the M lines was 0.20 keV. Similarly, in the work of Backenstoss *et al.*[26] the $3d$ splitting in lead appears to be larger by 0.27 keV than the calculated value, with a quoted error on the $M\alpha$ lines of 0.10 keV. This error refers, however, to the individual lines of the doublet, while the error of the doublet spacing is smaller, perhaps by a factor of 2.[27] A similar trend shows up in their results for bismuth where the discrepancy amounts to 0.29 keV with a quoted error for the individual lines of 0.25 keV, while the error on

TABLE V. M lines. Transition energies in keV.

	^{208}Pb	^{207}Pb	^{206}Pb	^{204}Pb
$4f_{7/2}$-$3d_{5/2}$	937.98± 0.06	937.83± 0.06	937.87± 0.06	937.99± 0.06
$4f_{5/2}$-$3d_{3/2}$	971.85± 0.06	971.83± 0.06	971.86± 0.06	971.86± 0.06
$5f_{7/2}$-$3d_{5/2}$	1366.52± 0.08	1366.42± 0.06	1366.40± 0.08	1366.57± 0.09
$5f_{5/2}$-$3d_{3/2}$	1404.74± 0.08	1404.66± 0.08	1404.62± 0.09	1404.68± 0.11
$6f_{7/2}$-$3d_{5/2}$	1599.67± 0.15	1599.68± 0.21	1599.11± 0.20	1599.80± 0.19
$6f_{5/2}$-$3d_{3/2}$	1639.98± 0.19	1640.23± 0.24	1639.92± 0.24	1640.21± 0.34
$3d$ splitting from $4f$-$3d$	43.07± 0.03	43.20± 0.03	43.19± 0.03	43.08± 0.03
$3d$ splitting from $5f$-$3d$	42.95± 0.10	42.98± 0.09	42.95± 0.10	42.84± 0.14
$3d$ splitting from $6f$-$3d$	43.04± 0.24	43.28± 0.31	43.53± 0.30	43.14± 0.39
$3d$ splitting from L lines	43.13± 0.18	43.25± 0.13	43.24± 0.36	43.13± 0.21
Weighted mean	43.06± 0.03	43.18± 0.03	43.17± 0.03	43.07± 0.03
χ^2/N	0.5	1.8	2.3	1.0
Splittings refitted from $4f$-$3d$ without constraint on the $4f$ splitting.				
$3d$ splitting	42.51± 0.23	42.87± 0.21	42.79± 0.23	42.46± 0.26
$4f$ splitting	8.64± 0.23	8.87± 0.21	8.80± 0.23	8.58± 0.26

The calculated values are: $\Delta 3d = 42.82$ keV, $\Delta 4f = 9.20$ keV.

TABLE VI. The 2*s* levels. Transition energies in keV.

	^{208}Pb	^{207}Pb	^{206}Pb	^{204}Pb
$2s_{1/2}$-$2p_{3/2}$	1030.44± 0.17	1030.02± 0.27	1029.99± 0.41	1028.83± 0.38
$2s_{1/2}$-$2p_{1/2}$	1215.43± 0.26	1215.60± 0.45	1215.58± 0.54	1214.12± 0.30
$3p_{3/2}$-$2s_{1/2}$	1507.48± 0.26	1508.71± 0.22	1509.53± 0.26	1511.63± 0.20
$2pfs$ splitt.	184.99± 0.31	185.58± 0.52	185.59± 0.68	185.29± 0.48

the doublet spacing is again probably only half as much.

Finally, we show in Table VI the three observed transitions involving the 2*s* level. From two of these transitions we can deduce the 2*p* fine-structure splittings which agree well with those deduced from the $K\alpha$ lines, see Table III, except for ^{204}Pb where the discrepancy is about $1\frac{1}{2}$ standard deviations.

There is good over-all agreement between the data presented here and other measurements on lead isotopes, in particular those presented in I. A comparison of the various measurements can be found in the compilation of Engfer *et al.*[28] The *K* lines in our new measurements are systematically lower than the ^{206}Pb, ^{207}Pb, and ^{208}Pb lines reported in I, but the discrepancy can be traced to a large extent to the revised value of the ^{16}O* calibration line which is lower than the value previously used by about 1 part in 10^4. Our new measurements of transitions to and from the 2*s* level differ somewhat from our old measurements in ^{206}Pb.[1] At the time, we obtained the values 1507.93 ±0.80 and 1217.81 ±0.80 for the $3p_{3/2}$-2*s* and 2*s*-$2p_{1/2}$ transitions, respectively. These are to be compared with the new values (from Table VI): 1509.53 ±0.26 and 1215.58 ±0.54. The difference is presumably due to improved data and a vastly improved calibration method.

V. ANALYSIS OF THE RESULTS

As a first step in the analysis we fitted the set of measured transition energies to a self-consistent set of energy levels. This was done mainly because the number of energy levels involved is less than half the number of transitions measured. The data used in the fit consisted of 16 transition energies for each isotope, namely, two $K\alpha$ lines, two $K\beta$ lines, three $L\alpha$ lines, six *M* lines, and three transitions involving the 2*s* level, a total of 64 measurements. These data were fitted to six energy levels ($1s_{1/2}$, $2p_{1/2}$, $2p_{3/2}$, $2s_{1/2}$, $3p_{3/2}$, $3d_{3/2}$) for each of the four isotopes, in addition to a common set of energies for the $3d_{5/2}$, $5f_{5/2}$, and $6f_{5/2}$ levels for which we ignored the isotope shifts. The $4f_{5/2}$ energies were arbitrarily fixed at the calculated value of 1201.17 keV for all four isotopes, as we did in I. The result of the fit is shown in Table VII. The χ^2 is 48.5 for 37 degrees of freedom. In Table VIII the isotope shifts (IS) of the lighter lead isotopes with respect to ^{208}Pb are listed for the lower muonic energy levels. For all higher levels, the isotope shifts are too small to be detected.

Next we analyzed the set of energy levels in terms of finite nuclear sizes. We used a conventional and straightforward method similar to that described in detail in I. An analysis of our data

TABLE VII. Self-consistent set of energy levels in keV.

Level	^{208}Pb	^{207}Pb	^{206}Pb	^{204}Pb
$1s_{1/2}$	10 593.13± 0.41	10 599.89± 0.43	10 604.34± 0.41	10 614.88± 0.41
$2p_{1/2}$	4815.14± 0.06	4815.96± 0.08	4817.19± 0.06	4818.62± 0.08
$2p_{3/2}$	4630.25± 0.05	4630.98± 0.06	4631.50± 0.05	4632.72± 0.06
$2s_{1/2}$	3599.75± 0.17	3600.81± 0.26	3601.54± 0.34	3604.14± 0.26
$3p_{3/2}$	2092.20± 0.32	2092.10± 0.34	2092.01± 0.39	2092.41± 0.33
$3d_{3/2}$	2173.01± 0.05	2173.00± 0.05	2173.02± 0.05	2173.03± 0.05
$3d_{5/2}$	2129.90± 0.04			
$4f_{5/2}$	1201.17 (fixed at calc. value)			
$4f_{7/2}$	1191.97 (fixed at calc. value)			
$5f_{5/2}$	768.23± 0.04			
$5f_{7/2}$	763.51± 0.04			
$6f_{5/2}$	533.01± 0.08			
$6f_{7/2}$	530.28± 0.08			
$\chi^2/N = 1.31$				

was published recently by Ford and Rinker[29] based on their generalized radial moment method. We present here the results of our direct approach which is more familiar to experimentalists and gives a good description with the smallest number of parameters.

We desribe the nuclear charge distribution using the usual two-parameter Fermi distribution

$$\rho(r)=\rho_0/\{1+\exp[n(r-c)/c]\} \quad (2)$$

with normalization, for charge Z,

$$\rho_0=(3Z/4\pi c^2)/(1+\pi^2/n^2)\ . \quad (3)$$

The so-called skin-thickness parameter t which represents the distance over which the density falls off from 90 to 10% of its central value, is related to the Fermi parameters n and c by the expression

$$t=(4c/n)\ln 3\ . \quad (4)$$

We also calculated the reduced radius r_0 which is related to the equivalent radius R_{eq}. The latter is the radius of a uniform charge distribution having the same rms radius as the Fermi distribution:

$$R_{eq}=(\tfrac{5}{3}\langle r^2\rangle)^{1/2}=r_0A^{1/3}\ . \quad (5)$$

The muonic energy levels were calculated numerically by solving the Dirac equation for a finite charge distribution with the lowest order vacuum polarization potential, of order $\alpha(Z\alpha)$, added to the electrostatic potential. The vacuum polarization potential used in this calculation was that given by Barrett *et al.*[30] using an expansion due to Glauber, Rarita, and Schwed[31] as described by McKee.[32]

The other corrections were treated as perturbations and added to the calculated Dirac energies. The higher order vacuum polarization corrections of order $\alpha^2(Z\alpha)$, $\alpha(Z\alpha)^3$, and $\alpha(Z\alpha)^n$ with $n>3$, were calculated for us by Sundaresan and Watson.[6] Their results agree with those published by Blomqvist[5] for the $4f$ and $5g$ levels of lead within a few eV, but apply to the lower levels as well. Recently, various authors[33-36] have calculated these vacuum polarization terms taking into account the finite nuclear size effect on these corrections. Most of these calculations apply to the higher levels of lead, such as $4f$ and $5g$, but Rinker and Wilets[33] also calculated the finite size effect for the lower levels. Their results suggest a sizable effect as compared to point nucleus values of the higher order vacuum polarization correction, up to about 0.5 keV for the $2p$-$1s$ transitions. Since Rinker and Wilets's calculations for individual level shifts include an undetermined integration constant, we have determined the corrections for the lower levels from their results by biasing their values so as to obtain the value 8 eV (attractive) for the $4f$ levels of lead as calculated by Arafune. No calculations were available for the $3p$ levels. We estimated the effect to be (40 ± 20) eV.

TABLE VIII. Isotope shifts in keV.

	IS(208-207)	IS(208-206)	IS(208-204)
$1s_{1/2}$	6.75 ± 0.17	11.20 ± 0.11	21.74 ± 0.11
$2p_{1/2}$	0.82 ± 0.09	2.05 ± 0.08	3.48 ± 0.10
$2p_{3/2}$	0.74 ± 0.08	1.26 ± 0.06	2.47 ± 0.07
$2s_{1/2}$	1.06 ± 0.31	1.79 ± 0.37	4.38 ± 0.31
$3p_{3/2}$	−0.10 ± 0.47	−0.19 ± 0.51	0.21 ± 0.46
$3d_{3/2}$	−0.01 ± 0.06	0.00 ± 0.06	0.02 ± 0.06

For the calculation of the muonic Lamb shift correction, we followed the method of Barrett *et al.*[30] The Lamb shift decreases the binding energy, typically by about 3 keV for the $1s$ state in lead. The calculation of the Lamb shift involves, however, a comparatively large uncertainty, about 30% according to the authors.[30]

The relativistic recoil corrections were taken from the work of Friar and Negele[37] and Barrett.[38]

The largest theoretical uncertainties, however, are those related to the calculation of nuclear polarization by the muon. This effect increases the binding energy of the muon and early estimates of this effect by Cooper and Henley[39] amounted to a relatively large correction, namely 58 keV for the $1s$ state in lead and possibly up to as much as 185 keV. Recent calculations[16,17,40] brought this correction down to about 6 keV, and they agree with each other within the rather large theoretical uncertainties. Experimentally, this effect was first established by Anderson *et al.*[15] and found to be in rough quantitative agreement with the most recent calculations. As described in the Introduction to the present paper, one of our objectives was to obtain additional information on the nuclear polarization effect and we will say more about this later.

The calculated energy levels and radiative corrections are listed in Table IX. The nuclear polarization corrections which we have used will be discussed later.

As mentioned before, we used a two-parameter Fermi distribution (2) to treat the finite size of the nucleus since we have found by previous experience[1] that this is adequate to describe muonic atoms. Electron scattering results by Heisenberg *et al.*,[41] however, seemed to indicate a nuclear charge distribution for lead which has a 7% central depression and falls off at the edge faster than the Fermi distribution. Their analysis of ^{208}Pb,

TABLE IX. Energy levels and radiative corrections of ^{208}Pb in keV (calculated for a two-parameter Fermi shape with $c = 6.650$ and $t = 2.311$).

Level	Finite nucleus energy	1st order vacuum polarizat.	Lamb shift	Higher order vac. pol. ($n \geq 2$)	Finite size eff. in h.o. vac. pol.	Relat. recoil corr.	Anom. magnetic moment	Electron screening	Total
$1s_{1/2}$	10519.58	67.11	−2.30	−0.38	0.36	0.38	−0.45	0.00	10584.30
$2p_{1/2}$	4781.24	32.36	−0.59	−0.28	0.14	0.11	0.24	0.01	4813.23
$2p_{3/2}$	4599.36	29.83	−0.45	−0.27	0.14	0.09	−0.21	0.01	4628.50
$2s_{1/2}$	3579.56	19.36	−0.63	−0.20	0.04	0.09	−0.07	0.02	3598.17
$3d_{3/2}$	2162.43	10.53	−0.02	−0.16	0.04	0.02	0.06	0.03	2172.93
$3d_{5/2}$	2120.34	9.87	−0.01	−0.15	0.04	0.01	−0.04	0.04	2130.10
$3p_{3/2}$	2081.33	10.25	−0.20	−0.13	(0.04)	0.03	−0.06	0.05	2091.31
$4f_{5/2}$	1197.38	3.78	0.00	−0.09	0.01	0.00	0.01	0.08	1201.17
$4f_{7/2}$	1188.31	3.67	0.00	−0.08	0.01	0.00	−0.01	0.08	1191.98

using 250 and 500 MeV electrons, can be expressed with the help of a three-parameter Fermi-type distribution with a parabolic depression,

$$\rho(r) = \rho_0(1 + wr^2/c^2)/\{1 + \exp[n(r/c - 1)]\} \ . \quad (6)$$

For the parameter w they found $w = 0.14 \pm 0.10$ from their electron scattering results alone. Using our ^{208}Pb measurements of the $K\alpha$ and $L\alpha$ energies as constraints, they obtained an even larger value, $w = 0.32$ (no error quoted). Since our new measurements include precise data on the $2s$ energies which, as pointed out before, are particularly sensitive to the interior of the nuclear charge distribution, we first analyzed our ^{208}Pb data to compare the two-parameter charge distribution (2) with the three-parameter distribution (6). The levels fitted are the $1s$, the two $2p$ levels, as well as $2s$ and $3p_{3/2}$. We did not include the $3d$ levels in the fit because of the anomalous $3d$ splitting which we discussed before. In our first attempt, the results of which are shown in Table X, we did not include nuclear polarization. Comparing the two-parameter fit with the three-parameter fit, we see that the latter does not provide any improvement and that furthermore the parameter w turns out to be very close to zero. In addition, χ^2 in both fits turns out to be very large, a clear indication that some important effect has been

TABLE X. Fit of experimental ^{208}Pb data (energies in keV).

Level	Expt. Energies	two-parameter fit without nuc. pol.	three-parameter fit without nuc. pol.	three-parameter fit nuc. pol. incl.
$1s_{1/2}$ [a]	10593.13 ± 0.41	10593.24	10593.28	10592.30
$2p_{1/2}$ [a]	4815.14 ± 0.06	4815.29	4815.31	4815.15
$2p_{3/2}$ [a]	4630.25 ± 0.05	4630.11	4630.12	4630.25
$2s_{1/2}$ [a]	3599.75 ± 0.17	3599.44	3599.45	3600.05
$3d_{3/2}$	2173.01 ± 0.05	2172.93	2172.94	2172.85
$3d_{5/2}$	2129.90 ± 0.04	2130.09	2130.10	2130.07
$3p_{3/2}$ [a]	2092.20 ± 0.32	2091.84	2091.86	2092.01
$4f_{5/2}$	1201.17 fixed	1201.17	1201.17	1201.17
$4f_{7/2}$	1191.97 fixed	1191.97	1191.98	1191.98
		Nuclear Parameters and χ^2.		
$1/n$		0.0747 ± 0.0007	0.0747 ± 0.0007	0.0770 ± 0.0009
n		13.38 ± 0.12	13.39 ± 0.12	12.99 ± 0.15
r_0		1.19734 ± 0.00013	1.19730 ± 0.00013	1.20000 ± 0.00029
w			0.002 ± 0.020	−0.064 ± 0.015
c		6.678 ± 0.007	6.677 ± 0.007	6.712 ± 0.011
t		2.192 ± 0.018	2.192 ± 0.017	2.271 ± 0.023
χ^2		19	19	0.48
χ^2/N		6.2	9.6	0.24

[a] Fitted levels.

TABLE XI. Nuclear polarization shift in muonic lead [from Skardhamar (Ref. 40)] (in keV, the negative sign means *increased* binding energy).

$1s_{1/2}$	−6.8 ± 2.0
$2s_{1/2}$	−1.6 ± 0.7
$2p_{1/2}$	−1.9 ± 0.3
$2p_{3/2}$	−1.8 ± 0.3
$3p_{3/2}$	−0.7 ± 0.2
$3d_{3/2}$	+0.03 ± 0.02
$3d_{5/2}$	0.00 ± 0.02

neglected.

As outlined in Sec. I, we found evidence in our previous work[1,15] that the introduction of nuclear polarization, especially in the $1s$ level, improves the agreement between the observed and calculated values of the energies to a great extent. We therefore attempted a three-parameter fit, including the nuclear polarization corrections as calculated by Skardhamar[40] (see Table XI), whose calculations, although considerably improved over previous estimates, still show uncertainties large compared to the precision achieved in the experimental measurements. These theoretical uncertainties had to be folded in with the experimental errors when the fit was made, so that the fit was largely constrained by the theoretical errors alone, and the results were therefore much less significant. This is unfortunate, but probably unavoidable at the present stage. The last column in Table X shows the results of a three-parameter fit where the theoretical nuclear polarizations with their errors were taken into account. The resulting small value of χ^2 shown at the bottom of the table should not be considered as a very significant improvement in view of the large errors used. The important point we wish to make is that this calculation results again in a small value of w and that, furthermore, this parameter turns out to be negative. This would produce a slight enhancement at the center of the nuclear charge distribution, in contrast to the central depression suggested by Heisenberg *et al.*[41] We therefore concluded that there was no compelling evidence for w to be significantly different from zero and we proceeded to use the two-parameter Fermi distribution (2) for the remainder of the analysis.

At this point is is perhaps worthwhile to comment on the high precision with which the parameter r_0 can be determined (one to three parts per 10^4, according to the model). This is due to the high sensitivity of the binding energies to a variation of this parameter, as illustrated by the corresponding derivatives, such as $\delta E_{1s}/\delta r_0 \simeq -4600$ keV/fm at $r_0 \simeq 1.2$ fm. It is also fair to say, however, that from one model to another the variation in r_0 can be an order of magnitude larger as the examples in Table X clearly show.

TABLE XII. Nuclear parameter fit. Results of a two parameter fit to four energy levels (marked by *). Nuclear polarization from Table XI is included in the fitted levels. The errors used in the fit are compounded from the experimental errors and theoretical uncertainties. The last line shows $\delta E(1s)$, the difference between the calculated energy (*not* including nuclear polarization) and the experimental energy of the $1s_{1/2}$ level.

Quantity	^{208}Pb	^{207}Pb	^{206}Pb	^{204}Pb
$1/n$	0.0791 ± 0.0006	0.0787 ± 0.0005	0.0778 ± 0.0018	0.0785 ± 0.0013
n	12.64 ± 0.10	12.70 ± 0.07	12.86 ± 0.29	12.74 ± 0.22
c (fm)	6.650 ± 0.007	6.647 ± 0.005	6.649 ± 0.019	6.627 ± 0.014
t (fm)	2.311 ± 0.016	2.299 ± 0.012	2.272 ± 0.045	2.287 ± 0.034
r_0 (fm)	1.2005 ± 0.0001	1.2011 ± 0.0001	1.2016 ± 0.0003	1.2030 ± 0.0003
$\langle r^2 \rangle^{1/2}$ (fm)	5.5097 ± 0.0006	5.5036 ± 0.0004	5.4970 ± 0.0015	5.4857 ± 0.0012
χ^2/N	0.11	0.05	0.73	0.47
	δE = calc. energy−expt. energy (in keV)			
Level	The value in parentheses is $\lvert\delta E\rvert$/total error			
$2p_{1/2}$*	0.00 (0.0)	0.03 (0.1)	−0.20 (0.6)	−0.06 (0.2)
$2p_{3/2}$*	0.05 (0.2)	−0.06 (0.2)	0.15 (0.4)	−0.02 (0.1)
$2s_{1/2}$*	0.00 (0.0)	−0.04 (0.1)	0.20 (0.3)	0.02 (0.0)
$3p_{3/2}$*	−0.19 (0.4)	0.12 (0.3)	0.46 (0.9)	0.42 (1.0)
$3d_{3/2}$	−0.09 (1.5)	−0.07 (1.4)	−0.07 (1.4)	−0.06 (1.3)
$3d_{5/2}$	0.20 (4.1)	0.21 (4.2)	0.22 (4.3)	0.22 (4.3)
$\delta E(1s)$	−8.8 ± 1.2	−10.1 ± 1.1	−9.0 ± 2.8	−7.3 ± 2.2

The next step of the analysis followed the pattern of our original work on nuclear polarization.[1,15] The nuclear parameters n and c of the distribution (2) were determined from a fit to the levels from $2p$ upwards, leaving out the $1s$ level where the predicted nuclear polarization and its error are large. We then used the nuclear parameters so determined to calculate the energy of the $1s$ level and compared it to the experimental value. The difference $\delta E(1s)$ was then attributed tentatively to a nuclear polarization correction to the $1s$ energy to be compared to the theoretical estimates of this effect. Contrary to our previous work, however, we included the nuclear polarization as calculated by Skardhamar[40] into the theoretical values of the higher levels and folded the theoretical uncertainties in with the experimental errors. The higher levels which we fitted were: $2p_{1/2}$, $2p_{3/2}$, $2s_{1/2}$, and $3p_{3/2}$. We again excluded the d levels from the fit for the reasons outlined previously.

The results of this study are shown in Table XII. The nuclear polarization corrections $\delta E(1s)$, which we obtained for the $1s$ level, are shown in the last line of the table. They turn out to be only slightly larger than, but not inconsistent with, the predicted value of -6.8 ± 2.0 keV. For ^{206}Pb, where the nuclear polarization correction is now -9.0 ± 2.8 keV, we had previously[15] obtained the value -6.8 ± 2.3 keV. The difference is due to changes in our analysis, such as the inclusion of higher order vacuum polarization and nuclear polarization in the theoretical energies, rather than to improved experimental measurements. Similarly, the new result has a somewhat larger error which originates from the inclusion of nuclear polarization with its theoretical uncertainty into the higher energy levels.

It should be noted that the error we quote on $\delta E(1s)$ is a combination of the experimental error on the $1s$ energy (see Table VII), theoretical errors (mainly the Lamb shift), and errors resulting from the fitted nuclear parameters.

For ^{208}Pb we obtain -8.8 ± 1.2 keV. This compares with the value -12.5 ± 0.8 keV obtained by Jenkins *et al.*[18] These authors also quote a lower value, -8.9 ± 2.7 keV, obtained by fitting simultaneously for the nuclear polarization in the $1s$ and $2s$ levels. In this case, their nuclear polarization for the $2s$ level comes out at -0.6 ± 0.7 keV, somewhat lower than the predicted value of -1.6 ± 0.7 keV.

Our evidence so far supports the view that nuclear polarization is present in roughly the amount predicted by theoretical calculations. To check to what extent our results depend on the chosen method of analysis, we have also tried various other approaches. For instance, we have fitted our data to the calculated energies without including nuclear polarization corrections in the higher levels. In another attempt, we did include these corrections, but disregarded the theoretical errors, using only the experimental errors in the fitting procedure. Although we found that the results of these attempts varied somewhat in detail, as can be expected, we still obtained values for $\delta E(1s)$ in the interval -5 to -10 keV for all four lead isotopes. This seems to indicate that our evidence for nuclear polarization is unlikely to be the result of our particular method of analysis. It is true, however, that the radial moment analysis of our data by Ford and Rinker[29] shows a smaller effect, namely, only 2–4 keV. According to these authors it is even possible to fit the $1s$ state nearly exactly without destroying the fit to the other transitions. This is probably due to the fact that their larger number of parameters allows more flexibility. Since the experimental errors are already much smaller than the theoretical uncertainties, it is likely that further progress in this field must wait for more accurate theoretical calculations. Finally, we would like to stress the fact that our evidence for nuclear polarization is strongly dependent on our ability to measure the weak transitions leading to and from the $2s$ level.

We have not included the $3d$ levels in our fitting process. We can, however, use the nuclear parameters obtained to calculate the theoretical values of these levels. It turns out that, for all four isotopes, the experimental splitting is larger than the theoretical value by about 300 eV, the upper $3d_{5/2}$ level being shifted up by 60–90 eV, while the lower $3d_{3/2}$ level is shifted down by 200–220 eV. This result differs from our preliminary analysis which seemed to indicate that the anomaly affected mainly the $3d_{5/2}$ state, while the $3d_{3/2}$ level seemed to be observed in its predicted position. The anomaly in the $3d$ splitting of the four lead isotopes varies from 240 ± 30 to 360 ± 30 eV with an average of 300 eV and is now well established with a significance of about 10 standard deviations. As mentioned in Sec. IV, some indication of the anomalous $3d$ splitting can already be found in earlier data.[1,23] We have no explanation for this anomaly.

The last point we have to consider is related to the nuclear parameters which are listed in Table XII. It is seen that the skin thickness parameter t turns out to be almost the same for all four isotopes. The rms radius $\langle r^2 \rangle^{1/2}$, on the other hand, increases monotonically going from ^{204}Pb to ^{208}Pb. However, it increases less than can be expected from the $A^{1/3}$ law, as illustrated by a simultaneous *decrease* of r_0. This tendency

of a slight increase in density as one approaches the doubly magic nucleus ^{208}Pb, which we observed previously for the isotopes 206-207-208, now applies equally well to the isotope 204. The actual values of the correlated parameters n and c differ somewhat from those quoted previously, due to the different method of analysis used, but the trend is the same.

As we have observed before, the values which we quote for r_0 are model-dependent. The trend displayed in Table XII is, however, significant insofar as the same model was used for the four isotopes. We have checked, furthermore, that this trend is insensitive to slight variations of the model.

VI. CONCLUSIONS

We have presented the results of an experiment to measure muonic x rays with high resolution from four separated lead isotopes 204, 206, 207, and 208. Some of the highlights of this experiment are summarized below.

A study of the line shapes did not show any anomaly. We were, however, able to detect a slight line broadening due to the natural linewidth.

The binding energies of the lower levels were measured in all four isotopes. These included the circular orbits up to the $6f$ doublet as well as the $2s_{1/2}$ and $3p_{3/2}$ states.

The $3d$ fine-structure splitting was shown to exhibit an anomaly which is so far unexplained. The experimentally measured splitting was found to be larger than the calculated value by about 300 eV (or about 10 standard deviations) in each one of the four isotopes.

Those lower levels which are strongly affected by the finite nuclear size could be adequately fitted with a two-parameter Fermi distribution of the nuclear charge, provided nuclear polarization is taken into account. This experiment therefore supports recent calculations of this effect. It is unfortunate, however, that the theoretical uncertainties in the predicted nuclear polarization corrections for the lower levels are, at present, much larger than the experimental errors, so that the constraints in fitting the experimental data to the theoretical values are not as tight as one would like. We therefore hope that our results will provide an incentive for theorists to calculate these corrections more accurately.

Finally, the analysis of our data shows that the nuclear density increases slightly in going from ^{204}Pb to ^{208}Pb, in agreement with a tendency observed in our previous work. The skin thickness parameter t, on the other hand, changes very little.

ACKNOWLEDGMENTS

We wish to thank Professor M. K. Sundaresan and Dr. P. J. S. Watson for many stimulating discussions and Professor Sundaresan and Mr. G. Hussain for performing certain calculations for us. We are indebted to Arnold Smith for programming the computer and Jean Legault and Paul Plowe for building the computer interfaces. The contributions of R. Armstrong, R. Gabriel, R. Ryan, D. Switzer, and M. Wenger in the fabrication and conducting of the experiment are also gratefully acknowledged. The U.S. Atomic Energy Commission kindly loaned to us the isotopically enriched lead.

---

*Research supported by the U.S. National Science Foundation and the National Research Council of Canada.

†Present address: National Research Council of Canada, Ottawa, Canada.

‡Present address: Lawrence Berkeley Laboratory, Berkeley, California.

§Present address: Carleton University, Ottawa, Canada.

[1]H. L. Anderson, C. K. Hargrove, E. P. Hincks, J. D. McAndrew, R. J. McKee, R. D. Barton, and D. Kessler, Phys. Rev. 187, 1565 (1969), henceforth referred to as I.

[2]On loan from the U.S. Atomic Energy Commission.

[3]D. Kessler, invited paper presented at the Muon Physics Conference, Fort Collins, Colorado, Sept. 6–10, 1971 (unpublished); Carleton University Report (unpublished).

[4]M. K. Sundaresan and P. J. S. Watson, Phys. Rev. Lett. 29, 15 (1972).

[5]J. Blomqvist, Nucl. Phys. B48, 95 (1972).

[6]M. K. Sundaresan and P. J. S. Watson, private communication; unpublished.

[7]C. K. Hargrove, in *Proceedings of the International Conference on Electromagnetic Sizes of Nuclei, Ottawa, Canada, 22–27 May 1967,* edited by D. J. Brown, M. K. Sundaresan, and R. D. Barton (Carleton University Press, Ottawa, Canada, 1968), p. 299.

[8]C. K. Hargrove, E. P. Hincks, G. R. Mason, R. J. McKee, D. Kessler, and S. Ricci, Phys. Rev. Lett. 23, 215 (1969).

[9]A. Steudel, Z. Physik 133, 438 (1952); see the review article by P. Brix and H. Kopfermann, Rev. Mod. Phys. 30, 517 (1958).

[10]R. B. Chesler and F. Boehm, Phys. Rev. 166, 1206 (1968).

[11]P. L. Lee and F. Boehm, Phys. Rev. C 8, 810 (1973).

[12]V. L. Fitch and J. Rainwater, Phys. Rev. 92, 789 (1953).

[13]D. Kessler, H. L. Anderson, M. S. Dixit, H. J. Evans,

R. J. McKee, C. K. Hargrove, R. D. Barton, E. P. Hincks, and J. D. McAndrew, Phys. Rev. Lett. 18, 1179 (1967).

[14]This particular figure is taken from a talk by H. L. Anderson, in *Proceedings of the International Conference on Electromagnetic Sizes of Nuclei* (see Ref. 7), p. 53, with the 2*s* wave function added. Similar curves, but without 2*s*, were used for the first time by Fitch and Rainwater (Ref. 12).

[15]H. L. Anderson, C. K. Hargrove, E. P. Hincks, J. D. McAndrew, R. J. McKee, and D. Kessler, Phys. Rev. Lett. 22, 221 (1969).

[16]R. K. Cole, Phys. Rev. 177, 164 (1969).

[17]Min-Yi Chen, Phys. Rev. C 1, 1167 (1970).

[18]D. A. Jenkins, R. J. Powers, P. Martin, G. H. Miller, and R. E. Welsh, Nucl. Phys. A175, 73 (1971).

[19]R. J. McKee, C. K. Hargrove, A. G. Smith, H. Mes, A. Thompson, and M. Dixit, Nucl. Instrum. Methods 92, 421 (1971).

[20]M. G. Strauss, F. R. Lenkszus, and J. J. Eichholz, Nucl. Instrum. Methods 65, 285 (1969).

[21]M. S. Dixit, H. L. Anderson, C. K. Hargrove, R. J. McKee, D. Kessler, H. Mes, and A. C. Thompson, Phys. Rev. Lett. 27, 878 (1971).

[22]M. S. Dixit, Ph.D. thesis, University of Chicago, 1971 (unpublished).

[23]C. W. Allen, *Astrophysical Quantities* (Athlone, Univ. of London, 1963), 2nd ed., p. 82.

[24]M. K. Sundaresan, private communication. We are indebted to M. K. Sundaresan and G. Hussain for performing these calculations for us.

[25]C. K. Hargrove, R. J. McKee, H. L. Anderson, M. S. Dixit, D. Kessler, H. Mes, and A. C. Thompson, Phys. Rev. D (to be published).

[26]G. Backenstoss, S. Charalambus, H. Daniel, Ch. von der Malsburg, G. Poelz, H. P. Hovel, H. Schmitt, and L. Tauscher, Phys. Lett. 31B, 233 (1970).

[27]G. Backenstoss, private communication.

[28]R. Engfer, H. Schneuwly, J. L. Vuilleumier, H. K. Walter, and A. Zehnder, Nucl. Data A (to be published).

[29]K. W. Ford and G. A. Rinker, Phys. Rev. C 7, 1206 (1973).

[30]R. C. Barrett, S. J. Brodsky, G. W. Erickson, and M. H. Goldhaber, Phys. Rev. 166, 1589 (1968).

[31]R. Glauber, W. Rarita, and P. Schwed, Phys. Rev. 120, 609 (1960).

[32]R. J. McKee, Phys. Rev. 180, 1139 (1969).

[33]G. A. Rinker and L. Wilets, Phys. Rev. Lett. 31, 1559 (1973); G. A. Rinker, private communication.

[34]J. Arafune, Phys. Rev. Lett. 32, 560 (1974).

[35]L. S. Brown, R. N. Cahn, and L. D. McLerran, Phys. Rev. Lett. 32, 562 (1974).

[36]M. Gyulassy, Phys. Rev. Lett. 32, 1393 (1974).

[37]J. L. Friar and J. W. Negele, Phys. Lett. 46B, 7 (1973).

[38]R. C. Barrett, D. A. Owen, J. Calmet, and H. Grotch, Phys. Lett. 47B, 297 (1973).

[39]L. N. Cooper and E. M. Henley, Phys. Rev. 92, 801 (1953).

[40]H. F. Skardhamar, Nucl. Phys. A151, 154 (1970).

[41]J. Heisenberg, R. Hofstadter, J. S. McCarthy, I. Sick, B. C. Clark, R. Herman, and D. G. Ravenhall, Phys. Rev. Lett. 23, 1402 (1969).